



## ORIGINAL ARTICLE

# Oil spill cleanup by raw flax fiber: Modification effect, sorption isotherm, kinetics and thermodynamics



Mohamed Ahmed Mahmoud

Chemical Engineering Department, College of Engineering, Jazan University, Jazan, Saudi Arabia

Received 2 January 2020; accepted 23 February 2020

Available online 29 April 2020

## KEYWORDS

Oil;  
Microwave;  
Flax fiber;  
Isotherm;  
Kinetics;  
Acetylation

**Abstract** Modification of raw flax fiber by acetylating process and microwave energy was useful in the application of oil spill cleanup. The change in fibers was characterized by scientific analysis (FTIR, SEM, XRD and contact angle). The results indicate that the modified fibers by the acetylating process have extra hydrophobic properties than both microwave radiation and raw fibers. Oil/Artificial seawater(3.5% salinity by NaCl) system (O/W-S) was used as a liquid phase operation system. Fast oil sorption was reached at 6 min and attained(equilibrium) at 10 min. Acetylated fiber (ACF)has higher oil sorption capacity(24.54 g/g) than both raw(13.75 g/g) and microwave fiber (17.42 g/g) with exothermic effect. The sorption kinetics and isotherms indicate that the oil sorption onto ACF agreement with pseudo second-order kinetic model and Freundlich isotherm model. Also, the economic reusing of fiber was evaluated. The process of acetylation demonstrated the ability to improve the absorptive properties of the fibers, which makes them able to compete with synthetic fibers in the oil spill cleanup and industrial applications, as well as cheap and eco-friendly due to their biodegradation.

© 2020 Published by Elsevier B.V. on behalf of King Saud University. This is an open access article under the CC BY-NC-ND license (<http://creativecommons.org/licenses/by-nc-nd/4.0/>).

## 1. Introduction

Oil spills are one of the greatest catastrophic environmental occurrences that lead to the damage of entire ecosystems and inflict the economy of the countries that have leaked oil (Likon et al., 2013). The occurrence of oil spills in water

environments represents the biggest problems facing the environment of the seas and oceans, due to the increase in oil extraction and production processes, and the use of giant tankers and thousands of cases happen yearly resulting from transportation and production, as well as cases of natural leakage at the bottom of the ocean (Fathy et al., 2018; Peng et al., 2018). Oil spills have damage effects on factories and oil refineries due to the risk of fires or explosions, as well as the biggest impact threatening desalination plants because drinking water can be mixed with toxic hydrocarbons, causing these plants to shut down and for periods that may be prolonged (Singh et al., 2013; Liu et al., 2018). Land leak cleaning operations are much easier than cleaning up

E-mail addresses: [mohnma55@gmail.com](mailto:mohnma55@gmail.com), [drchemeng@yahoo.com](mailto:drchemeng@yahoo.com)

Peer review under responsibility of King Saud University.



Production and hosting by Elsevier

oil spills on the surface of the water. There are several methods have been used to overcome the oil spill released in the water environment (Aleksandrs and Vladislavs, 2020; Gu et al., 2014; Wang et al., 2014; Wu et al., 2014; Xue et al., 2014). Biological treatment is carried out by using genetically modified microorganisms that they can live and feed on oil, so they analyze oil slicks and convert them to methane and carbon dioxide that are released into the atmosphere (Radetic et al., 2003; Abdul and Abdulrauf, 2012; Cui et al., 2014; Piperopoulos et al., 2019). Skimming or suction is done through sweepers or hoods installed on giant trawlers so that the oil is collected in tanks intended for that to be transported later to the oil refineries (Hubbe et al., 2013). Chemical treatment is used to disperse oil slicks, thereby reducing their effectiveness in blocking sunlight and air from surface marine organisms and causing them to fade in large areas (Ibrahim et al., 2010). Burning, where the fire is ignited to get rid of some stains far from the beaches or marine installations (Wahi et al., 2013; Liu and Wang, 2019). The use of barriers, which are floating chains that stand in the way of oil-laden water currents and prevent them from reaching the beaches or the important vital areas (Jude et al., 2016). Removal of oils using agriculture materials (absorption technique) is useful in ridding the environment from oil leakage and solid waste is used as fuel in some industrial processes such as steam boilers (Ngaini et al., 2014; Abdullah et al., 2010; Wang and Deng, 2019). Because of the cheap price, biodegradation, and the low density of natural fibers, it increased the tendency towards using natural fibers instead of synthetic fibers in the environment and industrial development (Aghareed et al., 2019). So numerous work was carried out to modify the surface of natural fibers and giving them new properties to replace synthetic fibers in many areas (Juliana and Raul, 2016). Several methods (chemical, physical techniques and functional nanoparticles decoration) have been used to modify the fiber surface, essentially to improve fire resistance, adhesion and hydrophobic properties, also to change inexpensive fibers into expensive materials (Zafer et al., 2020; Fulga et al., 2019). The plasma technique is a physical procedure that was carried out to modify the fiber surface by forming strong bonds between new functional groups and matrix of fibers which lead to increase the mechanical properties of natural fibers (Alberto et al., 2016; Alekseeva and Stepanova, 2019). Chemical modification was carried out by immersion the fibers in a chemical solution (alkali, peroxides, silane, water-repelling agents, etc) to remove the weak constituents of fiber (hemicelluloses and lignin) and hence improve the mechanical and adsorption performance of the fibers (Wei et al., 2020). Functional nanoparticles decoration technique has been developed to functionalize nanofiber surfaces with nanoparticles. Incorporation of nanoparticles into the surface of nanofibers gives new properties such as fluorescent and magnetic properties (Min et al., 2020; Lei et al., 2019). In this work, the modification of raw flax fibers by acetylation process and microwave radiation was analyzed and studied in the oil sorption from artificial seawater. Sorption isotherm, kinetics and thermodynamics were investigated. Also, the reusability of exhausted fibers was studied.

## 2. Materials & methods

### 2.1. Materials

Raw Flax fibers were obtained from the flax factory, Tanta, Egypt. Ethanoic anhydride, methylbenzene and perchloric acid were analytical grade and obtained from Sigma-Aldrich.

Used motor oil (Density: 706 kg/m<sup>3</sup>) collected from auto maintenance & repair operations and artificial seawater (3.5% salinity by NaCl) were used in experiments.

### 2.2. Preparation of flax fiber

Raw flax fibers (RF) were cut into < 1 cm parts and immersed in hot distilled water several times to eliminate foreign materials. Washing was continued until foreign materials were eliminated and clear effluent was achieved. Then, flax fibers were dried at 105 °C before modification processes.

**Acetylation modification:** Acetylated flax fibers (ACF) were prepared by immersed 5 g flax fiber in the mixture of acetylating liquid (200 ml methylbenzene, 100 ml ethanoic anhydride and 3 ml of perchloric acid as a catalyst) for 1 hr at 65 °C in a thermostatic water bath. Then, filtration and washing using distilled water were carried out to remove the remaining acetylating liquid and dried at 105 °C before used (Fig. 1).

**Microwave modification:** Microwaved flax fibers (MIF) were prepared by a microwave radiation technique in a microwave oven of (180–1000)W (Microwave Research & Applications, Inc. Model BP 090). Flax fibers were exposed to 450 W microwave energy for 7 min. Then cooled before using it.

### 2.3. Method

10 ml of used oil was added on 1L artificial seawater (3.5% salinity by NaCl) in a 1.5L glass container in the thermostatic shaker water bath at operating conditions 30 °C, 100 rpm, 1.0g of fiber was added in the system for time range (2–20 min), then separated, left to drain for 7 min, and re-weighting. Water sorbed with oil was determined by drying the wet (oil and water) fiber at 105 °C for 24 hrs. Water (W<sub>C</sub>) and oil sorption content (O<sub>C</sub>) were calculated by the following eqs.:

$$W_C \text{ (g)} = M_{(w+o)} - M_{D(o)} \quad (1)$$

$$O_C \text{ (g)} = M_{D(o)} - M_F \quad (2)$$

Where, M<sub>(w+o)</sub>, M<sub>D(o)</sub> and M<sub>F</sub> are the weights (g) of wet (oil and water) fiber, dried wet(oil) fiber and initial flax fiber, respectively.

The oil sorption percent (O<sub>S</sub>%) from the oil/water system was determined by the following eqs:

$$O_S \% = [M_{D(o)} - M_F / M_F] \times 100 \quad (3)$$

Oil sorption capacity q<sub>os</sub> (g of oil /g of flax fiber) can be calculated from the following eq.:

$$q_{os} = (M_{D(o)} - M_F) / M_F \quad (4)$$

$$q_{os} = O_C \text{ (g)} / M_F \text{ (g)} \quad (5)$$

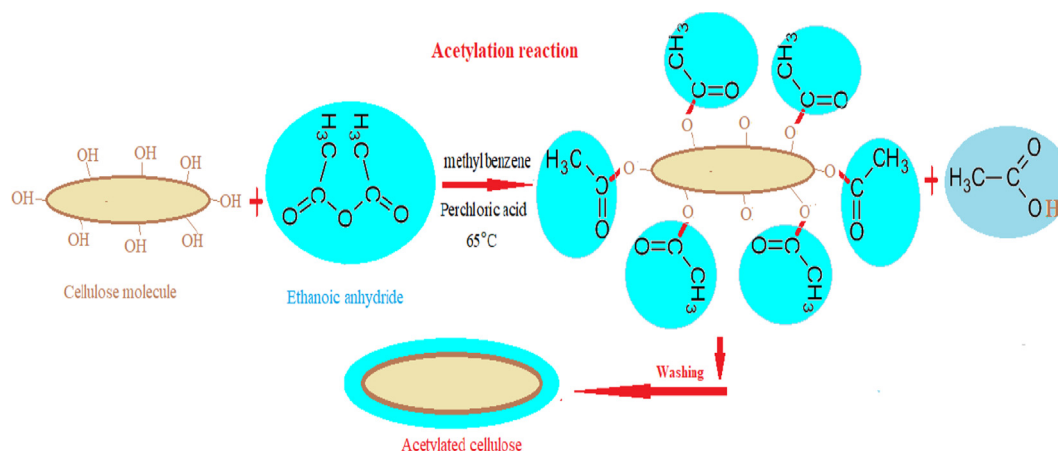


**Fig. 1** Acetylation process of flax fiber.

### 3. Results & discussion

#### 3.1. Characterization

Cellulose, hemicelluloses, and lignin are the main components of raw flax fiber (Ali et al., 2012). These components can sorb hydrophilic and hydrophobic liquids because they contain sites of both hydrophilic and hydrophobic and also due to the porous structure of the fibers. Cellulose components have a great affinity to hydrophilic than to hydrophobic substances (Abutaleb et al., 2020).

##### 3.1.1. SEM analysis

Fig. 2a indicates that the raw flax fiber surface was smooth and compact with very low pores. While low micropores or cavities on the surface of the fibers was appeared after modifying by microwave energy (Fig. 2b). After acetylation, the surface of fiber was rough and more micropores or cavities appeared due to the removal of hemicelluloses and lignin and hence increase the oil sorption storage (Fig. 2c) (Juliana and Raul, 2016).

##### 3.1.2. X-ray analysis

Fig. 3X shows the X-ray diagrams of raw (Fig. 3Xa) and modified flax fiber. The crystallinity properties of fiber were 50.12%, 49.04% and 35.98% for raw and microwaved and acetylated fibers. Fig. 3Xb shows that the fibers retain their crystalline nature with a small decrease in the intensity of the peaks after the fiber exposed to the microwave effect. While after the acetylation process, The crystalline nature was dropped due to the replacement of OH group by acid anhydride group which decrease the hemicellulose and lignin content (Vincenzo et al., 2019). Also, the intensity at  $2\theta = 25^\circ$  is much lower than the microwave effect and the peak at  $14 < 2\theta < 18^\circ$  becomes wider and less in the intensity. Also, a new peak at  $5 < 2\theta < 11^\circ$  attributes to cellulose acetate become visible (Fig. 3Xc) (Likon et al., 2013).

##### 3.1.3. FTIR analysis

Fig. 3Y demonstrates the FTIR spectrum of the raw, microwave radiation and acetylated fibers. The band at  $3484\text{ cm}^{-1}$  attributes to OH group and C-H group at  $2950\text{ cm}^{-1}$ . The wavenumbers at  $1720\text{ cm}^{-1}$  and  $1640\text{ cm}^{-1}$  attribute to

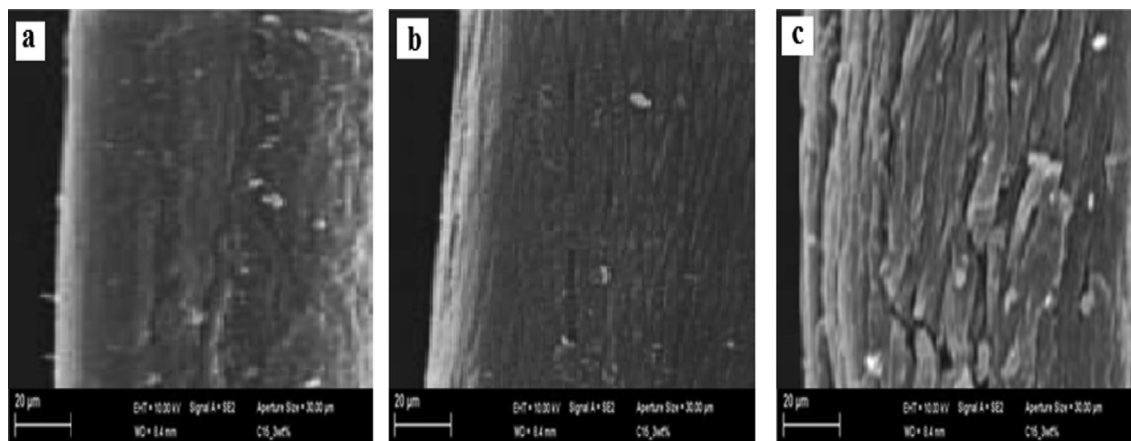


**Fig. 2** SEM of RF (a) MIF (b) and ACF (c).

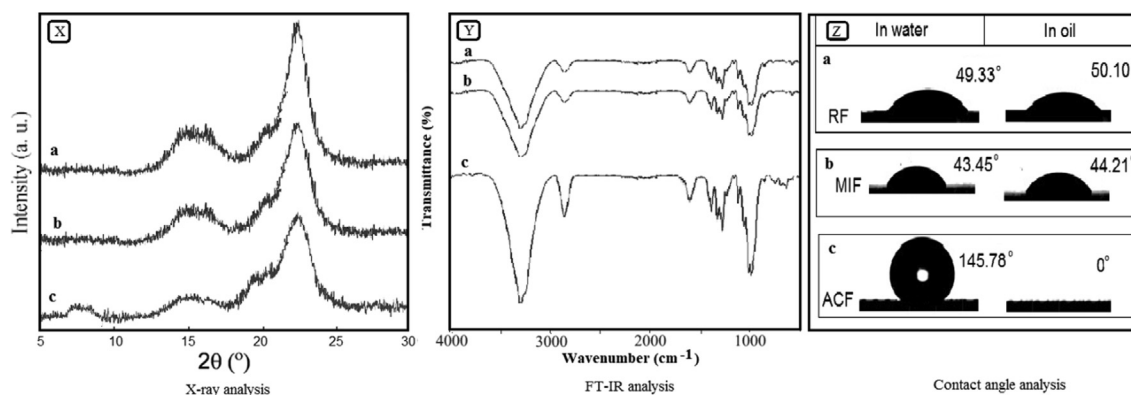


**Fig. 3** X-ray analysis of (RF (Xa) MIF (Xb) and ACF (Xc)), FTIR analysis of (RF (Ya) MIF (Yb) and ACF (Yc)) and contact angle analysis of (RF (Za) MIF (Zb) and ACF (Zc)).

C = O group (Abdullah et al., 2010). The wavenumbers at 1463 and 1435  $\text{cm}^{-1}$  refer to  $-\text{CH}$ ,  $-\text{CH}_2$  vibrations and C-H group at wave number 1385  $\text{cm}^{-1}$  of  $\text{CH}_3$  group. The wavenumbers at 1165–1130  $\text{cm}^{-1}$ , attribute to asymmetric C-O-C. The wavenumber at 1030  $\text{cm}^{-1}$  refers to C-O ether (Lim and Huang, 2007) (Fig. 3Ya). It was observed that the FTIR analysis of the microwave radiation fibers is approximately alike to raw fibers, indicating that there is no chemical change in the composition of fiber (Fig. 3Yb). The FTIR spectra of acetylated fibers show a rise in the intensity of the peaks due to the acetylation effect (Fig. 3Yc).

### 3.1.4. Contact angle analysis

Fig. 3Z shows the droplets of artificial seawater and used oil on the RF, MIF and ACF surface. Fig. 3Za and Zb show a low contact angle of RF (49.33°) and MIF (43.45°) in water and in oil (50.10°) and (26.12°), respectively which indicate the lipophilic and hydrophobic properties of RF and MIF. Whereas ACF has a contact angle of 145.78° in water and 0° in oil (Fig. 3Zc) indicating that the acetylation process increases the porous and hydrophobic structure of flax fiber and thus increase the oil sorption capacity from (O/W-S) system.

### 3.1.5. BET analysis

Brunauer-Emmett-Teller (BET) analysis indicates that RF has a surface area of 51.54  $\text{m}^2/\text{g}$  and a pore volume of 0.41  $\text{cm}^3/\text{g}$ , while MIF has a slight increase in the surface area of 52.66  $\text{m}^2/\text{g}$  and a pore volume of 0.433  $\text{cm}^3/\text{g}$ . But with ACF there is a more increase in the surface area and pore volume to 75.84  $\text{m}^2/\text{g}$  and 0.63  $\text{cm}^3/\text{g}$ , respectively due to the removal of weak constituents of hemicelluloses and lignin from the fiber structure by the chemical agents and hence improve the porous structure and sorption performance of the fibers (Juliana and Raul, 2016; Abutaleb et al., 2020).

### 3.2. Effect of the modification technique

The influence of the modification technique of flax fibers on the sorption capacity from artificial seawater, oil and oil/artificial seawater system was investigated under operating conditions (Table 1).

**Table 1** Effect of modification technique on sorption capacity of fibers.

Type of fibers	Assessment (AA)	Operating system	Sorption capacity (g/g)
Raw flax fibers (RF)	Water sorption assessment (W-AA)	(2 g fiber, 30C, 60 min, 1L artificial seawater and 100 rpm)	16.45
	Oil sorption assessment (O-AA)	(2 g fiber, 30C, 60 min, 1L oil and 100 rpm)	15.23
	Oil/water sorption assessment (O/W-AA)	(40 ml oil (39.32 g), 1L artificial sea water, 2 g fiber, 30C, 60 min and 100 rpm).	13.25
Acetylated flax fibers (RCF)	Water sorption assessment (W-AA)	(2 g fiber, 30C, 60 min, 1L artificial seawater and 100 rpm)	1.21
	Oil sorption assessment (O-AA)	(1 g fiber, 30C, 60 min, 1L oil and 100 rpm)	26.82
	Oil/water sorption assessment (O/W-AA)	(40 ml oil (39.32 g), 1L artificial seawater, 1 g fiber, 30C, 60 min and 100 rpm).	24.54
Microwaved flax fibers (MIF)	Water sorption assessment (W-AA)	(1 g fiber, 30C, 60 min, 1L artificial seawater and 100 rpm)	20.10
	Oil sorption assessment (O-AA)	(1 g fiber, 30C, 60 min, 1L oil and 100 rpm)	21.15
	Oil/water sorption assessment (O/-WAA)	(40 ml oil (39.32 g) in 1L artificial seawater at operating conditions (1 g fiber, 30C, 60 min and 100 rpm).	17.42

In the water sorption assessment (W-AA), Fig. 4a and Table 1 show that the water hydrophobicity is increased in the acetylated fiber (ACF) more than both raw (RF) and

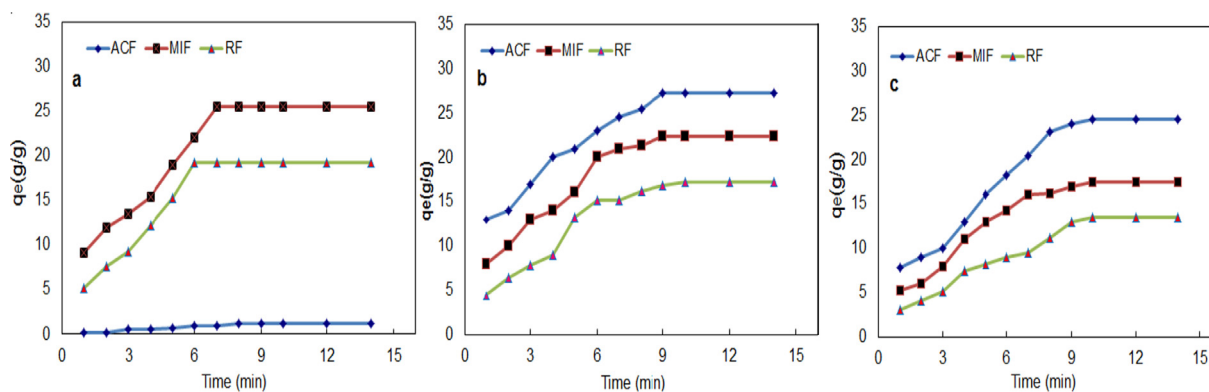


**Fig. 4** Sorption assessment of ACF, MIF and RF in (a) artificial sea water (b) oil (c) artificial seawater/oil at (25 ml oil/ 1 L artificial seawater system, 100 rpm 30 °C).

microwave radiation (MIF) fiber. The sorption capacities of artificial seawater are 1.21, 20.10 and 16.45 g/g for ACF, MIF, and RF, respectively. This indicates that the process of modification with ethanoic anhydride encapsulates the fiber with a layer resistant to the sorption of water, which earns the hydrophobic properties (Vincenzo et al., 2019; Reza et al., 2014). In the case of MIF, the increase in the water absorption rate more than RF is due to increased porosity as a result of exposure to microwave radiation (Jude et al., 2016; Mahmoud et al., 2016).

**In the oil sorption assessment (O-AA),** the oil sorption capacities are 26.82, 21.15 and 15.23 g/g for ACF, MIF and RF respectively (Table 1). The ACF has a rough, porous and hydrophobic surface acting as sorbing sites and increases the rate of oil sorption more than both RF and MIF. While the smooth and compacted surface of RF and low porosity of MIF led to reducing the oil sorption capacity. These explanations are confirmed by SEM analysis (Fig. 4b).

**In the oil/water sorption assessment (O/W-AA),** The results show an enhancement in the oil sorption capacity with ACF more than other fibers (MIF and RF) (Table 1). The process of treating the fiber with ethanoic anhydride increases the hydrophobic nature due to the reaction of the acid anhydride group in the ethanoic anhydride with the hydroxyl group in the cellulose molecules which causes the fiber to be coated with a hydrophobic film which leads to the packaging of fiber with a water-repellent layer that reduces water sorption when used in the oil removal from aqueous medium (Robabeh et al., 2016). Finally, ACF was found to be higher in oil sorption and lower water sorption followed by MIF and then RF (Fig. 4c) owing to the acetylation effect which enhances the hydrophobicity and surface roughness with enormous extent of pores which lead to finding more storage space for oil sorption in the fibers (Ting et al., 2014).

### 3.3. Sorption dynamics

The influence of the modification technique of flax fibers on the oil sorption capacity from the oil/artificial seawater system indicates that ACF has higher oil sorption capacity and lower water sorption followed by MIF and then RF. So that further studies were carried out using acetylated flax fibers (RCF).

#### 3.3.1. Sorption time effect and sorption mechanism

The effect of sorption time was determined in the range (1–20 min) by adding 1.0 g of ACF on 10 ml (9.83 g) in a 1L artificial seawater glass container at operating conditions (30 °C and 100 rpm). The obtained data shows that the percent of removal fast augmented with the rise of uptake time at 6 min ( $R\% = 92.88\%$ ) and became slow until an equilibrium state at 10 minutes ( $R\% = 99.98\%$ ) (Table 2) which shows that the oil sorption mechanism is fast at the initial period of oil sorption owing to the oleophilic contact and the capillary force of surface which increase the oil sorbed onto the fiber surface. After that oil can be sorbed into internal fiber pores by van der Waals forces (Ting et al., 2014; Wang et al., 2013). Whereas, the gradual increase in oil removal until the equilibrium state owing to the fullness of the sorption active sites of fibers (Ola et al., 2017; Mahmoud et al., 2016).

#### 3.3.2. Sorption dose effect

The effect of fiber dose on the oil sorption was investigated in the fiber dose range (0.5–3 g) by contact within 10 ml oil in a 1L artificial seawater at operating conditions (30 °C, 10 min and 100 rpm). Table 2 shows that with increasing the sorbent mass from 0.5 g to 1.0 g, the percent of oil removal increases from 61.37 to 99.99%, respectively which owing to the increase in the sorption sites in the fibers (Malakhov and Chvalun, 2019; Mahmoud et al., 2016). While the oil uptake capacity decreased from 12.276 to 3.276% for fiber dose of 0.5 to 3 g, respectively. Further increase in the fiber dose leads to a decrease in sorption capacity due to the aggregation of sorption sites. Consequently, as the fiber dose increased, the quantity of oil sorbed on a unit mass of ACF reduced, subsequent to a reduction in the sorption capacity.

#### 3.3.3. Effect of initial oil feed

Varying of initial oil quantity (10–35 ml) in 1L artificial seawater was used to study the effect of initial oil feed in the oil sorption capacity and removal percent using 1.0 g at operating conditions (30°C, 10 min and 100 rpm). The results (Table 2) indicate that oil removal is noticeably influenced with varying of initial oil feed in operating system where the removal percent declines from 99.98% to 71.41% and sorption capacity rises from 9.828 to 24.405 g/g for varying of initial oil feed

**Table 2** Dynamic parameters of oil sorption from artificial seawater by ACF.

Dynamic parameters		Sorption percent B <sub>p</sub> (%)	Sorption capacity q <sub>os</sub> (g/g)
<b>Time:</b>	2.0	65.72	6.460
(10 ml, 1.0 g, 20 min, 100 rpm, 30 °C)	4.0	77.31	7.599
	6.0	92.88	9.130
	8.0	94.45	9.284
	10.0	99.98	9.828
	12.0	99.98	9.828
	14.0	99.97	9.827
	16.0	99.98	9.828
	18.0	99.96	9.826
	20.0	99.98	9.828
<b>Initial oil concentration (g/L):</b> (1.0 g, 10 min, 100 rpm, 30 °C)	10 ml/l (9.83 g/L)	99.98	9.828
	15 ml/l (14.745 g/L)	99.98	14.742
	20 ml/l (19.66 g/L)	99.98	19.630
	25 ml/l (24.575 g/L)	99.98	24.571
	30 ml(29.490 g/L)	83.24	24.550
	35 ml(34.405 g/L)	71.41	24.405
<b>Adsorbent dose (g) :</b> (10 ml, 10 min, 100 rpm, 30 °C)	0.5	61.37	12.276
	1.0	99.98	9.828
	1.5	99.99	6.552
	2.0	99.99	4.914
	2.5	99.99	3.931
	3.0	99.99	3.276
	4.0	99.98	9.828
<b>Temperature (K) :</b> (10 ml, 10 min, 1.0 g, 100 rpm)	30 °C	97.93	9.626
	35 °C	88.31	8.680
	40 °C	71.85	7.062
	45 °C		

from 10 g/l to 35 g/l, respectively. The decrease in the oil sorption percent owing to the fullness of pores or storage space of fibers with oil which leads to a decrease in the sorption sites through an increase of oil feed quantity (Seema and Raz, 2020; Alaa et al., 2018).

### 3.3.4. Effect of temperature

Temperature is an important factor in the sorption of oils from the seawater owing to change the viscosity of oil and consequently the sorption capacity of sorbing materials. Table 2 shows that the oil sorption capacity decreases from 9.828 to 7.062g/g with increasing temperature from 30°C to 45°C, respectively. This is due to the decrease in the viscosity of the oil with the temperature gradient, which increases the oil solubility in water and thus the loss of oil sorbed from fiber during the draining step (Jun et al., 2020; Mahmoud et al., 2016).

### 3.4. Sorption kinetics

To estimate the sorption kinetics of oil uptake from oil/artificial seawater system onto acetylated flax fibers, pseudo-first order, pseudo-second order and Elovich kinetic models are investigated using a non-linear procedure which is a better method to determine the sorption kinetic parameters. The agreement of sorption models with experimental results was evaluated by chi-square analysis ( $\chi^2$ ) and correlation coefficient ( $R^2$ ). The terminologies of kinetic models, chi-square analysis ( $\chi^2$ ) and correlation coefficient ( $R^2$ ) are presented in the subsequent equations:

*Pseudo-first-order model* (Aghareed et al., 2019; Angelova et al., 2011).

$$q_t = q_e (1 - e^{-K_1 t}) \quad (6)$$

*Pseudo-second-order model* (Piperopoulos et al., 2019).

$$q_t = K_2 q_e^2 t / (1 + K_2 q_e t) \quad (7)$$

**Table 3** Results of oil sorption kinetic models at (25 ml oil/1L artificial seawater system, 100 rpm 30 °C).

Value	Sorption kinetic models	Experimental q <sub>e</sub> (mg/g)
24.571	<b>Pseudo-first-order kinetics</b>	
	q <sub>e</sub> (g/g)	36.99
	K <sub>1</sub> (L/min)	0.258
	R <sup>2</sup>	0.883
	χ <sup>2</sup>	2.750
	<b>Pseudo-second-order kinetics</b>	
	q <sub>e</sub> (g/g)	25.42
	K <sub>2</sub> (g/g.min)	0.0953
	R <sup>2</sup>	0.996
	χ <sup>2</sup>	0.129
<b>Elovich model</b>		
α (g/g.min)	2.665	
β (g/g)	12.93	
R <sup>2</sup>	0.914	
χ <sup>2</sup>	5.618	

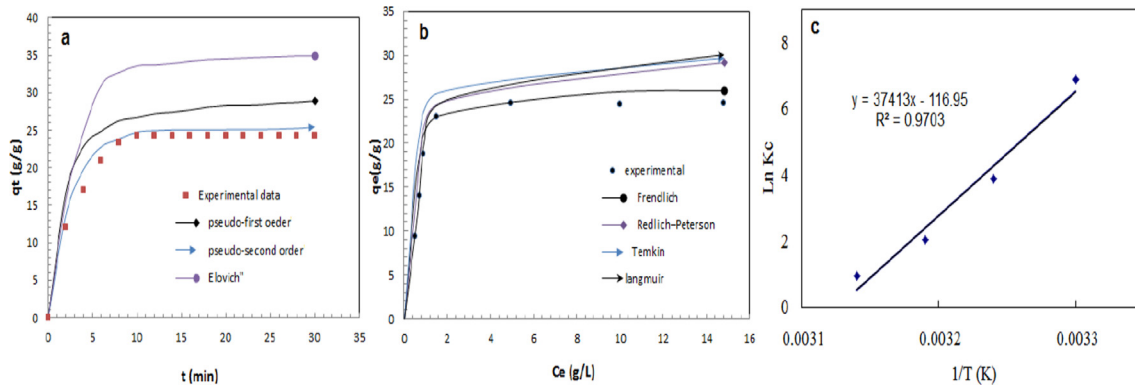


**Fig. 5** Sorption kinetic (a) and isotherm (b) models and thermodynamic (c) of oil sorption onto ACF at (25 ml oil/ 1 L artificial seawater system, 100 rpm 30 °C).

The Elovich kinetic model (Fathy et al., 2018; Angelova et al., 2011).

$$dq_t/dt = \alpha \exp(-\beta dt) \quad (8)$$

Where,  $q_e$  and  $q_t$  are the oil sorption capacity (mg/g) at equilibrium and time  $t$ .  $K_1$  (L/min) and  $K_2$  (g/mg.min) are the constants of pseudo-first order and pseudo-second order kinetic models, respectively. The  $\alpha$  and  $\beta$  are the constants Elovich model.

$$R^2 = \frac{\sum_{i=1}^n (q_e \text{ experimental} - q_e \text{ calculated})^2}{\sum_{i=1}^n (q_e \text{ experimental} - q_e \text{ calculated})^2 + \sum_{i=1}^n (q_e \text{ experimental} - q_e \text{ calculated})^2} \quad (9)$$

$$\chi^2 = \sum_{i=1}^n \frac{\sum_{i=1}^n (q_e \text{ experimental} - q_e \text{ calculated})^2}{q_e \text{ calculated}} \quad (10)$$

Table 3 shows the parameters of sorption kinetic models, which displays that the modeled sorption capacity (25.42 g/g) of pseudo-second-order kinetic model is agreement with experimental capacity with higher  $R^2$  (0.996) and lower  $\chi^2$  (0.329) values than the other models indicating that the pseudo-second-order kinetic model (Fig. 5a) is the agreement model for oil sorption onto ACF which suggested that the process of oil sorption is physical as well as chemical sorption in nature (Shobha et al., 2020; Angelova et al., 2011).

### 3.5. Sorption isotherm modeling

Isotherm models of Langmuir, Freundlich, Temkin and Redlich-Peterson (Table 4) were estimated to describe the equilibrium oil uptake on ACF by nonlinear systems (Zhu et al., 2009; Min et al., 2019). The isotherm studies can supply beneficial evidence on the sorption mechanism.

Fig. 5b illustrates the non-linear plot of isotherms at 30 °C and the sorption isotherm parameters are listed in Table 4. The results display that the Freundlich isotherm achieves the greatest fitting model for oil sorption onto ACF with greater correlation coefficient ( $R^2$ ) and lower chi-square analysis ( $\chi^2$ ) than other isotherms representing a multilayer oil sorption onto ACF (Wenling et al., 2019; Wang et al., 2019; Jing et al., 2019).

### 3.6. Sorption thermodynamics

Sorption thermodynamic study was used to determine the nature of oil sorption onto ACF. The change in enthalpy ( $\Delta H^\circ$ ), Free energy ( $\Delta G^\circ$ ) and entropy ( $\Delta S^\circ$ ), were calculated from the subsequent equations (Mahmoud et al., 2016).

$$\Delta G^\circ = -RT \log K_d \quad (11)$$

$$\Delta G^\circ = \Delta H^\circ - T\Delta S^\circ \quad (12)$$

$$\text{Ln} K_d = \Delta S^\circ / R - \Delta H^\circ / RT \quad (13)$$

**Table 4** Results of oil sorption isotherm models at (25 ml oil/ 1 L artificial seawater system, 100 rpm 30 °C).

Sorption isotherm	Nonlinear equation	Parameters	Value
Langmuir model	$q_e = \frac{Q_L K_L C_e}{1 + K_L C_e}$	$C_e$ = equilibrium oil concentration (g/L)	24.575 g/L
		$Q_L$ = constant (g/g)	30.45
		$K_L$ = constant (L/g)	15.479
		$R^2$	0.935
		$\chi^2$	5.042
Freundlich model	$q_e = K_F C_e^{1/n}$	$K_F$ = constant (g/g)	21.113
		$n$ = intensity of oil sorption	3.451
		$R^2$	0.984
		$\chi^2$	0.0781
		Temkin model	$q_e = \frac{RT}{H} \text{Ln}(K_T C_e)$
$H$ = constant (J/mol)	9.542		
$R$ = universal gas constant (J/mol/K)	8.314		
$T$ = temperature (K)	303		
$R^2$	0.781		
$\chi^2$	13.542		
Redlich-Peterson model	$q_e = \frac{K_{RP} C_e}{(1 + A C_e^\beta)}$		
		$A$ = constant (L/g) <sup><math>\beta</math></sup>	21.540
		$\beta$ = exponent of adsorption energy	0.7021
		$R^2$	0.934
		$\chi^2$	1.214

**Table 5** Thermodynamic parameters for the oil sorption by ACF.

Temperature (K)	$\ln K_c$	$\Delta G^\circ$ (KJmol <sup>-1</sup> )	$\Delta H^\circ$ (KJmol <sup>-1</sup> )	$\Delta S^\circ$ (KJmol <sup>-1</sup> .K <sup>-1</sup> )
303	6.88	-16.44	-311.051	-0.9723
308	3.87	-11.58		
313	2.02	-6.721		
318	0.936	-1.859		

$$K_c = q_{os}/C_e \quad (14)$$

Where  $q_{os}$ ,  $C_e$ ,  $T$  and  $R$  are equilibrium oil sorption capacity(g/g), equilibrium oil concentration(g/l), and  $R$  are temperature (°C) and gas constant (8.314 J/mol.K), respectively. Van't Hoff plot (Fig. 5c) was used to determine the thermodynamic parameters (Table 5). The results indicate that the oil sorption procedure tends to be spontaneously sorption from the oil/water system. The negative value of  $\Delta G^\circ$  decreases with the temperature increase from 30 °C to 45 °C indicating the favorability of oil sorption. The negative  $\Delta H^\circ$  denotes to exothermic sorption. Positive  $\Delta S^\circ$  denotes to decrease in the randomness of oil sorption onto fibers (Zhu et al., 2009; Abutaleb et al., 2020).

### 3.7. Economic studies

#### 3.7.1. Recover and recycle system

The economic procedure of oiled fiber squeezing by the roller system at 100 N.cm<sup>-2</sup> was employed to determine the oil recovery and the reusability of fiber (Radetic et al., 2003). The oil recovery percent ( $O_{RP}\%$ ) is determined by squeezing 5 g of the fiber after oil sorption from the oil/water system by the following eq.:

$$O_{RP}\% = [(M_{D(o)} - M_{sq}) / (M_{D(o)} - M_F)] \times 100 \quad (15)$$

Where,  $M_{sq}$  is the weights (g) of oil after squeezing system.

Fig. 6 shows that both oil sorption capacity was decreased with increasing sorption- squeezing cycles. After 6 cycles, the efficiency of fibers was declined below 50%, which indicates

that the acetylated flax fiber shows excellent reusability up to 6 cycles due to existence of acetyl group on the surface which is very useful to increase its reusability in the oil sorption from the (O/W-S) system.

#### 3.7.2. Recycle of exhausted fibers

After 6 cycles of oil sorption- squeezing process, the fibers became exhausted and useless in reusing them again in the sorption process and becoming solid residues causing pollution to the environment. Therefore, because the exhausted fiber contains a quantity of oil, it can be used as a solid fuel for some operations such as steam production in boilers. Resulting mass (Fly ash) produced from the burning process can be used as a new sorbent for oil and heavy metals (Ani et al., 2020; Radetic et al., 2003). The results of the operating conditions and optimum parameters of using fly ash in the oil and U (VI) sorption process in Table.6 indicate that fly ash resulting from the burning of exhausted fibers give a good oil and U(VI) ion removal percent reached to 95 and 97.45%, respectively. Good recycling of oiled fly ash can be carried out by burning to produce thermal energy and the resulting mass (fly ash) can be recycled in the sorption of both oil and heavy metal.

### 3.8. Comparison study

The Comparison between acetylated flax fiber and other sorbent materials of the same nature (Table.7) showed that the acetylated flax fiber has been demonstrated to have high sorption potential in the application of oil-water separation, with a

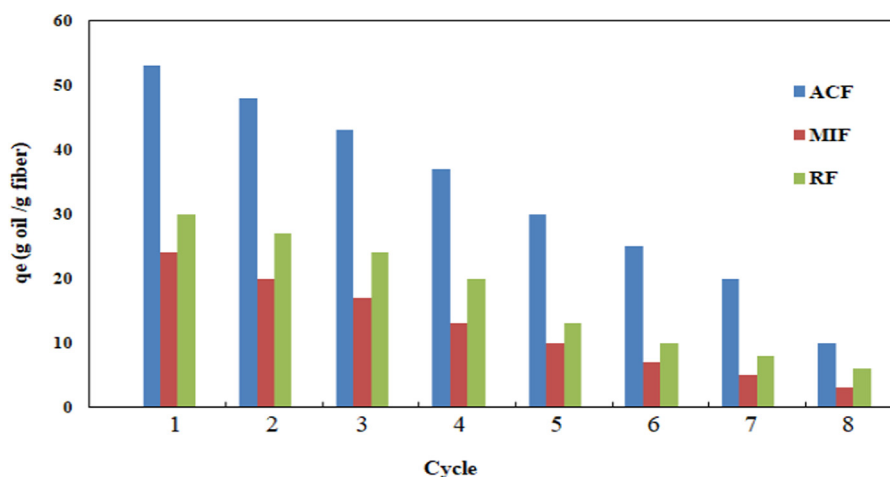


**Fig. 6** Sorption- squeezing cycle on the oil sorption capacity of ACF, MRF and RF in the oil/ artificial seawater system.

**Table 6** Operating conditions of oil and Heavy metal sorption process using fly ash (particle size is 70 mm).

Type of test	Operating conditions	Range	Optimum value of parameter	R%	Sorption Capacity
<b>Oil sorption test</b>					
10 ml oil/1L (O/W)	Time range (min)	2–15	5		
100 rpm	Dose range (g)	0.1–3	2	95.01	4.66(g/g)
	Temperature range (°C)	30–45	30(Exothermic)		
<b>Heavy metal sorption test</b>					
10 mg/L U(VI), 100 rpm	pH	2–7	4		
	Time range (min)	10–100	40	97.45	3.24(mg/g)
	Dose range (g)	0.1–2	0.3		
	Temperature range (°C)	30–45	45(Endothermic)		

**Table 7** Comparison between RF, MIF, ACF and other sorbent materials.

Sorbents	Sorption capacity (g /g)	Reference
Banana peel	7.0	(Alaa et al., 2018)
Cotton fibers	37.9	(Mohamed et al., 2013)
Rice husk	10	(Galblaub et al., 2015)
Saw dust	8.5	(Galblaub et al., 2015)
Corn cob	7.0	(Galblaub et al., 2015)
Bagasse	6.0	(Ahmed et al., 2005)
Barley straw	12.0	(Hussein et al., 2009)
Wheat straw	4.0	(Sirdas et al., 2014)
ACF	24.54	Present study
MIF	17.42	Present study
RF	13.25	Present study

some of the advantages, including fast removal rates, high sorption capacity and better surface chemistry. Also, the oil sorption capacities of RF and MIF have an acceptable value in a comparison with banana peel, rice Husk, saw dust, corn cob, bagasse, barley straw and wheat straw. The overall results appeared that flax fibers can be used in oil spill cleanup whether as raw fiber or after modification.

#### 4. Conclusions

The processing of flax fibers using microwave energy and ethanoic anhydride leads to a change in the sorption properties of flax fibers. The treatment of fiber with ethanoic anhydride leads to an increase in the hydrophobicity and porous structure of the fibers due to an interaction with the acid anhydride group of ethanoic anhydride. The microwave effect increases the porous formation of the fibers and thus increases the oil sorption but lower than acetylated fibers. ACF is less water and higher oil sorption followed by MIF and then RF from (O/A-S) system in the exothermic sorption effect. The sorption kinetics and isotherms indicate that the oil sorption onto ACF agreement with pseudo second order kinetic model and Freundlich isotherm model. Flax fiber has economical reusing in the oil sorption process. The rapid removal, cheap, biodegradable and better sorption capacity of the ACF make it a very suitable alternative sorbent mass for the oil from oil/water system.

#### References

- Abdul, Aziz A., Abdulrauf, A.M., 2012. Enamul H. A sustainable approach to controlling oil spills. *J. Environ. Manage.* 113, 213–227.
- Abdullah, M., Rahmah, A.U., Man, Z., 2010. Physicochemical and sorption characteristics of Malaysian Ceiba pentandra (L.) Gaertn. as a natural oil sorbent. *J. Hazard. Mater.* 177, 683–691.
- Abutaleb, A., Aghareed, M.T., Mahmoud, M.A., Daher, A.M., Desouky, O.A., Rania, F., Omer, Y.B., 2020. Removal and recovery of U(VI) from aqueous effluents by flax fiber: Adsorption, desorption and batch adsorber proposal. *J. Adv. Res.* 22, 153–162.
- Aghareed, M.T., Rania, F., Olfat, A.M., Maha, A.T., 2019. Oil spill clean-up using combined sorbents: a comparative investigation and design aspects. *Int. J. Environ. Anal. Chem.* 100, 311–323.
- Ahmed, B., Seyed, F.A., Ahmed, M., Reza, G.V., 2005. Oil spill cleanup from seawater by sorbent material. *Chem. Eng. Technol.* 28, 1525–1528.
- Alaa, E.G., Amer, A.A., Malsh, G., Hussein, M., 2018. Study on the use of banana peels for oil spill removal. *Alex. Eng. J.* 57, 2061–2068.
- Alberto, L. S., Edson C. B., Konstantin G. K., Mario U., Leide L. G., S., 2016. Carbon fiber surface modification by plasma treatment for interface adhesion improvements of aerospace composites, *Adv. Mater. Res.* 1135, 75–87.
- Aleksandrs, U., Vladislavs, Z., 2020. Oil Spill Detection Using Multi Remote Piloted Aircraft for the Environmental Monitoring of Sea Aquatorium. *Environmen. Climate Technol.* 24, 1–22.
- Alekseeva, A.A., Stepanova, S.V., 2019. Effect of Plasma Surface Modification of Mixed Leaf Litter on the Mechanism of Oil Film Removal from Water Bodies. *Russ. J. Gen. Chem.* 89, 2763–2768.
- Ali, N., El-Harbawi, M., Jabal, A.A., Yin, C.Y., 2012. Characteristics and oil sorption effectiveness of kapok fibre, sugarcane bagasse and rice husks: oil removal suitability matrix. *Environ. Technol.* 33, 481–486.
- Angelova, D., Uzunov, I., Uzunova, S., Gigova, A., Minchev, L., 2011. Kinetics of oil and oil products adsorption by carbonized rice husks. *Chem. Eng. J.* 172, 306–311.
- Ani, J.U., Akpomie, K.G., Okoro, U.C., Aneke, L.E., Onukwuli, O. D., Ujam, O.T., 2020. Potentials of activated carbon produced from biomass materials for sequestration of dyes, heavy metals, and crude oil components from aqueous environment. *Appl. Water Sci.* 10 (69), 2–11.
- Cui, Y., Xu, G., Liu, Y., 2014. Oil sorption mechanism and capability of cattail fiber assembly. *J. Ind. Text.* 43, 330–337.
- Fathy, M., El-Sayed, M., Ramzi, M., Abdelraheem, O.H., 2018. Adsorption separation of condensate oil from produced water using ACTF prepared of oil palm leaves by batch and fixed bed techniques. *Egypt. J. Pet.* 27, 319–326.
- Fulga, T., Mădălina, Z., Carmen-Alice, T., Mărioara, N., Asim S., 2019. Modified hemp fibers intended for fiber-reinforced polymer

- composites used in structural applications—A review. I. Methods of modification. *Polymer composite*.41,5-31.
- Galblaub, O.A., Shaykhiev, I.G., Stepanova, S.V., Timirbaeva, G.R., 2015. Oil spill cleanup of water surface by plant-based sorbents: Russian practices. *Process Saf. Environ. Prot.* 15, 1–15.
- Gu, J., Jiang, W., Wang, F., Chen, M., Mao, J., Xie, T., 2014. Facile removal of oils from water surfaces through highly hydrophobic and magnetic polymer nanocomposites. *Appl. Surf. Sci.* 301, 492–499.
- Hubbe, M.A., Rojas, O.J., Fingas, M., Gupta, B.S., 2013. Cellulosic substrates for removal of pollutants from aqueous systems: a review. 3. Spilled oil and emulsified organic liquids. *BioResources* 8, 3038–3097.
- Hussein, M., Amer, A.A., El-Maghraby, A., Taha, N.A., 2009. Availability of barley straw application on oil spill cleanup. *Int. J. Environ. Sci. Technol.* 6, 123–130.
- Ibrahim, S., Wang, S., Ang, H.M., 2010. Removal of emulsified oil from oily wastewater using agricultural waste barley straw. *Biochem. Eng. J.* 49, 78–83.
- Jing, Z., Min, Z., Teng, M., Jingxia, Y., Jingli, X., Njud, S.A., Muhammad, W., 2019. Anchoring nickel nanoparticles on three-dimensionally macro-/mesoporous titanium dioxide with a carbon layer from polydopamine using polymethylmethacrylate microspheres as sacrificial templates. *Mater. Chem. Front.* 3, 224–232.
- Jude, C.O., Edith, B.A., Victor, O.A., Friday, G.O., 2016. Kinetic studies of surface modification of lignocellulosic *Delonix regia* pods as sorbent for crude oil spill in water. *J. Appl. Res. Technol.* 14, 415–424.
- Juliana, C., Raul, F., 2016. Surface modification of natural fibers: a review. *Procedia Eng.* 155, 285–288.
- Jun, Z., Xiaoyu, C., Yuhuan, Z., Hongjing, T., Qingjie, G., Xiude, H., 2020. Efficient removal of oil pollutant via simultaneous adsorption and photocatalysis using La–N–TiO<sub>2</sub>–cellulose/SiO<sub>2</sub> difunctional aerogel composite. *Res. Chem. Intermed.* 46, 1805–1822.
- Lei, D., Min, Z., Jing, Z., Jingli, X., Njud, S.A., Muhammad, W., 2019. Fabrication of ultrafine nickel nanoparticles anchoring carbon fabric composites and their High catalytic performance. *Colloids Surf., A* 562, 146–153.
- Likon, M., Remskar, M., Ducman, V., Svegl, F., 2013. Populus seed fibers as a natural source for production of oil super absorbents. *J. Environ. Manage.* 114, 158–167.
- Lim, T.T., Huang, X., 2007. Evaluation of hydrophobicity/oleophilicity of kapok and its performance in oily water filtration: comparison of raw and solvent-treated fibers. *Ind. Crop Prod.* 26, 125–134.
- Liu, J., Wang, X., 2019. A New Method to Prepare Oil Adsorbent Utilizing Waste Paper and Its Application for Oil Spill Clean-up. *Bio Resources* 14, 3886–3898.
- Liu, Y., Peng, Y., Zhang, T., Qiu, F., Yuan, D., 2018. Superhydrophobic, ultralight and flexible biomass carbon aerogels derived from sisal fibers for highly efficient oil/water separation. *Cellulose* 25, 3067–3078.
- Malakhov, S.N., Chvalun, S.N., 2019. Preparation of Nonwoven Materials for Removal of Oil Spills from Water by Electrospinning of Polylactide Melt. *Russ. J. Appl. Chem.* 92, 1487–1491.
- Mohamed, H., Amer, A.A., Hoda, F.Z., Safaa, M.A., Mohamed, E., Mahmoud, N., 2013. Agricultural waste as a biosorbent for oil spills. *Int. J. Develop.* 2, 127–135.
- Mahmoud, M.B., Wanlin, H., Haoyi, L., Yumei, D., Weimin, Y., 2016. Temperature effect on sorption capacity of PP melt electrospun ultrafine fibers in marine oil spill clean up. *Trans. Tech. Publications Switzerland* 717, 104–111.
- Min, Z., Lei, D., Jing, Z., Libin, L., Hamed, A., Marwan, A.K., Jingli, X., 2020. Surface modification of carbon fibers with hydrophilic Fe<sub>3</sub>O<sub>4</sub> nanoparticles for nickel based multifunctional composites. *Appl. Surface Sci.* 509, 145348.
- Min, Z., Teng, M., Jing, Z., Jingli, X., Hadi, M.M., 2019. Oriented-assembly of hierarchical Fe<sub>3</sub>O<sub>4</sub>@CuSiO<sub>3</sub> microchains towards efficient separation of histidine-rich proteins. *Microporous Mesoporous Mater.* 286, 207–213.
- Ngaini, Z., Noh, F., Wahi, R., 2014. Esterified sago waste for engine oil removal in aqueous environment. *Environ. Technol.* 35, 2761–2766.
- Ola, A., Samir, M.N., Walaa, M.T., 2017. Palm fibers and modified palm fibers adsorbents for different oils. *Alexandria Eng. J.* 56, 749–755.
- Peng, Y., Yu, Z., Li, F., Chen, Q., Yin, D., Min, X., 2018. A novel reduced graphene oxide-based composite membrane prepared via a facile deposition method for multifunctional applications: oil/water separation and cationic dyes removal. *Sep. Purif. Technol.* 200, 130–140.
- Piperopoulos, E., Calabrese, L., Mastronardo, E., Abdul Rahim, S.H., Proverbio, E., Milone, C., 2019. Assessment of sorption kinetics of carbon nanotube-based composite foams for oil recovery application. *J. Appl. Polym. Sci.* 136, 47374.
- Radetic, M.M., Jovic, D.M., Jovancic, P.M., Petrovic, Z.L., Thomas, H.F., 2003. Recycled wool-based nonwoven material as an oil sorbent. *Environ. Sci. Technol.* 37, 1008–1012.
- Reza, B., Bagher, A., Nematollah, J.H.F., Masoome, F., 2014. Crude oil layer sorption from saline water surface by raw and acetylated sugarcane Bagasse. *Sci. Int.* 226, 1157–1161.
- Robabeh, A., Nasiman, B.S., Mohamed, H.I., Saeid, K., 2016. Acetylation of oil palm empty fruit bunch fiber as an adsorbent for removal of crude oil. *Environ. Sci. Pollut. Res.* 23, 11740–11750.
- Shobha, M., Spero, G., Dongyang, Deng, Lifeng, Zhang, 2020. Oil absorption capability of electrospun carbon nanofibrous membranes having porous and hollow nanostructures. *Mater. Lett.* 262, 127069.
- Seema, S., Raz, Jelinek, 2020. Solar-mediated oil-spill cleanup by a carbon dot-polyurethane sponge. *Carbon* 160, 196–203.
- Sidiras, D., Batzias, F., Konstantinou, I., Tsapatsis, M., 2014. Simulation of auto-hydrolysis effect on adsorptivity of wheat straw in the case of oil spill cleaning. *Chem. Eng. Res. Des.* 92, 1781–1791.
- Singh, V., Kendall, R.J., Hake, K., Ramkumar, S., 2013. Crude oil sorption by raw cotton. *Ind. Eng. Res.* 52, 6277–6281.
- Ting, D., Fumei, W., Guangbiao, X., 2014. Theoretical and experimental study on the oil sorption behavior of kapok assemblies. *Ind. Crops Prod.* 61, 325–330.
- Vincenzo, F., Elpida, P., Luigi, C., 2019. Assessment of *Arundo donax* Fibers for Oil Spill Recovery Applications. *Fibers* 7, 75.
- Wahi, R., Chuah, L.A., Choong, T.S.Y., Ngaini, Z., Nourouzi, M.M., 2013. Oil removal from aqueous state by natural fibrous sorbent: an overview. *Sep. Purif. Technol.* 113, 51–63.
- Wang, G., Zeng, Z.X., Wu, X.D., Ren, T.H., Han, J., Xue, Q.J., 2014. Three-dimensional structured sponge with high oil wettability for the clean-up of oil contaminations and separation of oil-water mixtures. *Polym. Chem.* 5, 5942–5948.
- Wang, J., Zheng, Y., Wang, A., 2013. Coated kapok fiber for removal of spilled oil. *Mar. Pollut. Bull.* 69, 91–96.
- Wang, N., Deng, Z., 2019. Synthesis of magnetic, durable and superhydrophobic carbon sponges for oil/water separation. *Mater. Res. Bull.* 115, 19–26.
- Wang, N., Qiong, Wen, Libin, Liu, Jingli, X., Jing, Zheng, Mingbo, Yue, Abdullah, M.A., Hadi, M.M., Min, Z., 2019. One dimensional hierarchical nanoflakes with nickel-immobilization for high performance catalysis and histidine-rich protein adsorption. *Dalton Trans.* 48, 11308–11316.
- Wenling, H., Xiaohui, G., Jing, Z., Jingli, X., Tasawar, H., Njud, S.A., Min, Z., 2019. Structural Evolution and Compositional Modulation of ZIF-8-Derived Hybrids Comprised of Metallic Ni Nanoparticles and Silica as Interlayer. *Inorg. Chem.* 58 (11), 7255–7266.
- Wei, Z., Pei, Y., Yizhong, C., Peijing, Y., Minzhi, C., Xiaoyan, Z., 2020. Evaluation of fiber surface modification via air plasma on the

- interfacial behavior of glass fiber reinforced laminated veneer lumber composites. *Constr. Build. Mater.* 233, 117315.
- Wu, L., Zhang, J.P., Li, B.C., Wang, A.Q., 2014. Mechanical- and oil-durable superhydrophobic polyester materials for selective oil absorption and oil/water separation. *J. Colloid Interf. Sci.* 413, 112–117.
- Xue, Z., Cao, Y., Liu, N., Feng, L., Jiang, L., 2014. Special wettable materials for oil/water separation. *J. Mater. Chem. A* 2, 2445–2460.
- Zafer, Y., Lutfiye, A., Mehmet, S., 2020. Effect of surface modification of carbon fibers on properties of carbon/epoxy composites. *Emerging Mater. Res.* 9, 1–9.
- Zhu, C., Wang, L., Chen, W., 2009. Removal of Cu(II) from aqueous solution by agricultural by-product: Peanut hull. *J. Hazard. Mater.* 168, 739–746.